


Positron-impact scattering off 1-1 $C_2H_2F_2$ from 0.1 eV to 4 keVAjay Kumar Arora ^{*}*Department of Physics, Keshav Mahavidyalaya, University of Delhi, Delhi-110034, India*Vardaan Sahgal and Anand Bharadvaja [†]*Department of Physics, Bhaskaracharya College of Applied Sciences, University of Delhi, New Delhi-110075, India*Kasturi Lal Baluja [‡]*Department of Physics and Astrophysics, University of Delhi, Delhi-110007, India*

(Received 11 January 2021; revised 1 August 2021; accepted 3 August 2021; published 19 August 2021)

Positron-impact cross sections of 1-1- $C_2H_2F_2$ are reported in the energy range from 0.1 to 4000 eV. The multicenter Gaussian-type orbitals were expanded within a single determinant Hartree-Fock self-consistent field scheme to obtain molecular wave function. The elastic cross sections were computed within fixed nuclei approximation by invoking the single center expansion approach. The target interactions were described by their local nature. The direct ionization and electron excitation cross sections were estimated using the binary-encounter-Bethe model for positron and scaled-Born approximation, respectively. The experimental scattering data were corrected to account for the angular discrimination effects. The corrections enhanced experimental measurements substantially in the low-energy range. The elastic cross sections are in an excellent agreement with the forward angle corrected total cross sections below positronium formation. The cross sections obtained by summing the elastic and inelastic cross sections incoherently were in good agreement with the experimental results. An in-depth analysis of the angular limitation of spectrometers employed in measuring the positron impact scattering cross sections and corrections arising out of the polar molecule are an integral part of the study. Some key aspects of electron and positron scattering are also discussed.

DOI: [10.1103/PhysRevA.104.022816](https://doi.org/10.1103/PhysRevA.104.022816)**I. INTRODUCTION**

1,1-difluoroethylene (1-1- $C_2H_2F_2$), commonly known as vinylidene fluoride (VDF), is an important industrial gas which contributes negligibly to global warming [1]. Though the electron-VDF scattering is investigated theoretically [2–4] and experimentally [4,5], the collision study of VDF from positron has largely remained neglected. The understanding of positron collision physics is essential for academic and technological development. It is well known that the positron scattering cross sections are required to model positron plasmas [6], transport phenomenon [7–12], interactions in astrophysical conditions [13], positron emission tomography [14], and characterization of materials [15,16].

The lack of positron impact collision data and the complexities involved in modeling the collision phenomenon can be possible reasons for the scattering process from VDF to remain unprobed. The theory of positron scattering is more complicated than electron scattering, even in the absence of exchange effects due to positronium (Ps) formation channel and strong polarization effects caused by the attraction between the positron and target electrons. The positronium is an electron-positron bound-state formation and occurs at energy 6.8 eV below ionization potential. The close-coupling

(CC) based *ab initio* methods like the molecular convergent close coupling (CCC) [17], time-dependent close coupling (TDCC) [18], and *R* matrix with pseudostates (RMPS) [19,20] are well established techniques to study positron scattering from atomic and molecular targets. These methods are, however, complicated as well as computationally demanding, and have been applied to several atoms, hydrogen molecule, and hydrogen molecular ion to study positron scattering [21–26]. Several other approaches have also been used to study the positron scattering [27]. The present study is aimed at exploring alternate methods which are simple both in the formulation and computation in comparison to *ab initio* methods and still provide reliable results for many-electron molecular targets in the least expensive way.

1,1-difluoroethylene is of special interest as it has intramolecular forces which are intermediary of pure hydrocarbon (C_2H_4) and pure perfluorocarbon (C_2F_4). These molecules bear identical hybridization and molecular structure except for H atoms in hydrocarbons which F atoms replace in 1,1- $C_2H_2F_4$ and C_2F_4 . The physicochemical properties of the targets primarily govern the scattering at energies below the ionization threshold. The target 1,1-difluoroethylene is weakly polar, whereas the other two are nonpolar [28]. The experimental value of polarizability is available only for C_2H_4 but the isotropic polarizability of all these targets is nearly the same [28]. Thus the outcome of the structural changes resulting from the substitution of F atoms for H atoms in hydrocarbons would be interesting in analyzing the scattering cross sections. The present positron

^{*}Permanent address: Presently on leave.[†]Corresponding author: anand_bharadvaja@yahoo.com[‡]Former address.

induced scattering from 1,1-difluoroethylene is a step forward to evaluate scattering dynamics from C_2H_4 and C_2F_4 . For this, a comprehensive set of positron induced collision data is required. To the best of our knowledge, the positron scattering data from C_2F_4 is unavailable, whereas only the total cross sections (TCS) are available for C_2H_4 and VDF [29].

Makochekanwa *et al.* measured positron impact TCS of 1-1- $C_2H_2F_2$ using a retarding potential time-of-flight apparatus [5] in the energy range from 0.4 to 1000 eV. However, the authors did not include any correction due to angular discrimination of the spectrometer or forward angle scattering effect [30]. In the absence of corrections, the measured cross sections (elastic or total) for any polar molecule are always less than their true values [31,32]. The experimental data must be therefore corrected before making a comparison with the theoretical results. The procedure to correct collision data requires the knowledge of the energy-dependent angular discrimination of the spectrometer and differential cross section (DCS) [29,30]. This crucial information is unavailable for several targets, including the present one. An alternative approach, independent of the DCS, is proposed to estimate the correction cross sections. This approach can be applied to several polar molecules for which experimental data exists in uncorrected form [29].

The positron impact cross sections like elastic DCS, elastic (ECS), and momentum transfer (MTCS) are reported by invoking the symmetry adapted single center expansion (SCE) technique [33,34] and using local potential approximation. The Born closure technique is applied to account for the long-range effects arising from the polar nature of the molecule [35]. The Born corrected ECS below Ps threshold are in excellent agreement with the theoretically corrected experimental results of Makochekanwa *et al.* [5]. The contribution from open channels like electron excitation and direct ionization is determined separately. The direct ionization cross sections are reported using the binary-encounter-Bethe (BEB) model for positron as proposed by Fedus and Karwasz [36]. The positron impact electron-excitation cross sections are estimated using the scaled-Born approximation of Kim [37]. The TCS estimated by summing the elastic and inelastic cross sections are in good accord with the forward angle corrected scattering TCS of Makochekanwa *et al.* except for the energy range between 4 and 30 eV. It is so because we have not considered the contribution of the Ps to the scattering process.

Additionally, we have examined the angular discrimination effect of linear type spectrometers used at the University of Trento and Australian National University (ANU) to measure the positron scattering data. Several other aspects of the positron and electron scattering from VDF are also discussed to lend credence to our work. It may be noted that scattering calculations are based on considering a molecule as an entity without invoking the independent atom model (IAM) approximation [38].

II. METHOD AND DETAILS

A. Elastic cross sections

The target wave function in the present symmetry-adapted SCE scheme is described by a single determinant (SD) HF approach within the self-consistent field (SCF) model. Thus

only the ground state is considered to represent the target wave function. The SD-HF approach leads to the static formulation of the scattering model. The representation of the polarization term is crucial in positron scattering rather than for electron scattering as it is the only attractive contribution to the positron-target interaction to counteract the repulsive nature of the static potential. The dynamical response of the target to the impinging positron is therefore included explicitly via addition of a local, energy-independent correlation-polarization (V_{cp}) potential. This explains the scattering in static-polarization approximation. The repulsive static potential represents the electrostatic interaction between the incident positron and the undeformed molecular charge distribution of the target. It is calculated exactly from the target electronic density obtained from a HF wave function. The long- and short-range regions of V_{cp} are matched at some distance (r_o) for the correct description of correlation polarization. The V_{cp} is represented as

$$V_{cp}(\vec{r}) = \begin{cases} V_{\text{corr}}(\vec{r}) & \text{for } r \leq r_o, \\ V_{\text{pol}}(\vec{r}) & \text{for } r > r_o. \end{cases} \quad (1)$$

The V_{corr} given by Perdew and Zunger [39] is used in the present calculations:

$$V_{\text{corr}}(\vec{r}) = \begin{cases} (0.0311 + 0.00133 r_s) \ln r_s \\ -0.0084 r_s - 0.0584 & \text{for } r_s < 1.0, \\ \frac{\gamma(1 + \frac{7}{6} \beta_1 r_s^{1/2} + \frac{4}{3} \beta_2 r_s)}{(1 + \beta_1 r_s^{1/2} + \beta_2 r_s)^2} & \text{for } r_s \geq 1.0, \end{cases} \quad (2)$$

where $\gamma = -0.1423$, $\beta_1 = 1.0529$, $\beta_2 = 0.3334$, and $r_s = [3/4\pi\rho(r)]^{1/3}$. The V_{pol} is of the form

$$V_{\text{pol}}(\vec{r}) = -\frac{1}{2r^6} \sum_{i,j} x_i x_j \alpha_{ij}, \quad (3)$$

where $r^2 = x_1^2 + x_2^2 + x_3^2$ and α_{ij} is the polarizability tensor.

The total interacting potential in positron-target interaction is, therefore, given by the sum of static and correlation-polarization potentials:

$$V(\vec{r}) = V_{st}(\vec{r}) + V_{cp}(\vec{r}). \quad (4)$$

In SCE, quantitylike potential (V_{st} or V_{cp}) is expanded around the center of mass (c.m.) of the N -electron molecular target:

$$V(\vec{r}) = \sum_{lm} V_{lm}(r) X_{lm}^{p\mu}(\theta, \phi). \quad (5)$$

Similarly the bound-state wave function in expanded form is given by

$$u_i(\vec{r}) = \frac{1}{r} \sum_{l,h} u_{i,hl}(r) X_{hl}^{p\mu}(\theta, \phi), \quad (6)$$

where μ is a component of the p th irreducible representation (IR) for a particular type of point group in ground state, h denotes a specific basis for a given partial wave l for μ , i is the specific multicenter orbital contributing to the density of bound electrons, r is the distance from the c.m. of the molecule, and $u_{i,hl}$ is the radial coefficient. The $X_{lh}^{p\mu}(\theta, \phi)$ are the symmetry adapted angular functions satisfying orthonormality conditions and are expressed as a linear combination

of spherical harmonics $S_{lm}(\theta, \phi)$:

$$X_{lh}^{p\mu}(\theta, \phi) = \sum_{m=-l}^{+l} b_{lhm}^{p\mu} S_{lm}(\theta, \phi). \quad (7)$$

The coefficients b_{lhm} corresponding to a particular IR are given by the character table in [40]. The spherical harmonics are constructed as a sum over a single index lm , with $h = 1$. For the closed-shell nonlinear molecules, $p\mu = A_1$.

The local formulation of scattering equations in terms of partial waves is then given by the following expression:

$$\left[\frac{d^2}{dr^2} - \frac{l(l+1)}{r^2} + k^2 \right] \psi_{lh}^{p\mu}(r) = 2 \sum_{l'h'} V_{lh, l'h'}^{A_1}(r) \psi_{l'h'}^{p\mu}(r), \quad (8)$$

where $k^2/2$ is the collision energy, $\psi_{l'h'}^{p\mu}(r)$ are the radial continuum wave function of the positron, and $V_{lh, l'h'}(r)$ is the local potential coupling element which is given by

$$V_{lh, l'h'}^{A_1}(r) = \int d\hat{r} X_{lh}^{p\mu}(\hat{r}) V(\vec{r}) X_{l'h'}^{p\mu}(\hat{r}). \quad (9)$$

Solving the equation under proper boundary conditions results in T -matrix elements from where the elastic cross sections are obtained in a body-fixed frame (BF):

$$\sigma_e^{BF} = \frac{\pi}{k^2} \sum_{lh} \sum_{l'h'} |T_{lh, l'h'}|^2. \quad (10)$$

Even though 1-1-C₂H₂F₂ is weakly polar in nature, a correction is nevertheless required to properly account for its long-range nature [35]. This is done via the Born top-up formula [41–44]. The Born corrected ECS in BF frame are then given by

$$Q_e^{BF} = \sigma_e^{BF} + \delta^B, \quad (11)$$

where

$$\delta^B = Q^B - Q_L^B. \quad (12)$$

Here, δ^B refers to the Born correction, Q^B is the cross sections obtained under full Born approximation, and Q_L^B indicates Born cross sections for L partial waves.

The quantity of prime interest in scattering is the differential cross section. The DCS for polar molecules in a fixed nuclei approximation (FNA) are divergent due to a singularity in the forward direction. Also, the partial wave expansion of DCS shows convergence issues. A closure formula is applied to overcome these problems [35]:

$$\frac{d\sigma}{d\Omega}(J\tau \rightarrow J'\tau') = \frac{d\sigma^B}{d\Omega} + \sum_{L=0}^{L_{\max}} (A_L - A_L^B) P_L(\cos\theta). \quad (13)$$

Here, A_L is the scattering coefficient [40]; $P_L(\cos\theta)$ is a Legendre polynomial and is a function of scattering angle θ . The first and the last term stands for the DCS obtained for a rotating and fixed dipole, respectively, within the first Born approximation. The L_{\max} represents the maximum number of partial waves of the continuum positron included in scattering calculations. The summation over L converges rapidly because the contributions from the higher partial waves to the DCS are dominated by the positron-dipole interaction, which

is calculated in Born approximation. The sum over the final rotor state ($J'\tau'$) gives rotationally unresolved DCS.

The corresponding expressions for the integral cross section or momentum transfer cross sections in the LAB frame (LF) are given by

$$Q_e^{LF} = \sigma_{e,rd}^B + \sigma_e^{BF} - \sigma_{e,fd}^B, \quad (14)$$

$$Q_M^{LF} = \sigma_{M,rd}^B + \sigma_M^{BF} - \sigma_{M,fd}^B. \quad (15)$$

The individual term on the right-hand side refers to cross sections (e : integral; M : momentum transfer) computed within Born approximation for a rotating dipole, in the FNA-BF (short-range interactions), and cross sections for a fixed dipole. Equation (13) is regarded as a correction to Born approximation treatment of the dipole interaction since it includes short-range effects from the BF calculations. The elastic cross sections represent the strength of forward scattering and the momentum transfer cross sections measure the average forward momentum lost in the collision. The momentum transfer cross sections provide a useful description of the motion of charged particles in a gas at a given temperature and computation of several collision quantities [45,46]. The POLYDCS [47] code employs this Born closure scheme to compute the Born corrected cross sections.

B. Direct ionization cross sections

A complete description of positron scattering requires the two-center close-coupling method in which the expansion is carried over the target and the Ps eigenstates [23–25]. The methods such as the molecular CCC and TDCC can accurately calculate total ionization cross sections across the entire intermediate-energy region. These highly advanced theories involve the use of large basis sets, complicated equations, and complex algorithms. The calculations require enormous computational resources, which make theoretical studies based on CCC methods and their variants highly expensive. Therefore, these methods cannot be applied easily to complex molecular systems. Compared to CC methods, the formulation and working of the BEB model is extremely easy as it does not require any fitted parameters, large basis sets, and bound and continuum wave functions. A simple analytical formula expresses the ionization cross sections in the BEB model and provides results across the entire intermediate-energy region in quick time, even for complex molecular targets. This model requires input parameters like the binding energies (B), orbital energies (U), and the occupation numbers (N) of the occupied orbitals, which can be obtained from standard quantum chemistry codes. In the BEB model, total ionization cross sections due to positron impact are obtained by summing the individual cross sections over the N occupied molecular orbitals [36]:

$$Q_I(t) = \sum_i^N Q_i^{e^+}(t_i), \quad (16)$$

where

$$Q_i^{e^+}(t_i) = \frac{S}{t_i + \gamma} \left[\frac{Q}{2} \left(1 - \frac{1}{t_i^2} \right) \ln t_i + (2 - Q) \left(1 - \frac{1}{t_i} \right) \right] \quad (17)$$

and

$$\gamma = u + 1 + \frac{C}{(t_i - 1)^{1.65}}, \quad (18)$$

Here, $t_i = E/B_i$, $u_i = U_i/B_i$ are the normalized energies $S = 4\pi a_0^2 N_i (R/B_i)^2$. R , B_i , U_i , and N_i refer to the Rydberg energy, binding energy, orbital kinetic energy, and the orbital occupation number, respectively, of the i th orbital; a_0 is the Bohr's radius. The term $t_i + \gamma$ represents a scaling factor and is chosen to make results consistent with Wannier law for positrons [48]. The constants C and Q are normally taken as unity. The exact value of C for a specific target can be derived only if reliable positron cross sections are available [36]. $Q = 1$ helps to make BEB model independent of differential oscillator strengths [49]. It is pertinent to mention that the positron impact direct ionization cross sections of H_2 obtained from the BEB model (with C and $Q = 1$) [36] are very much consistent with the two-center expansion calculations performed by Utamuratov *et al.* [50]. The scattering system in the molecular CCC model was represented by a total of 142 eigenstates (139 of target and 3 of Ps). These are the most accurate and highly expensive *ab initio* calculations performed to date for H_2 .

C. Excitation cross sections

The BE-scaled excitation cross sections are given by [37]

$$Q_{ex} = \frac{E}{E + B + E_{th}} \sigma_B, \quad (19)$$

where E is the incident positron energy, B is the binding energy of the valence molecular orbital, E_{th} is the excitation threshold energy, and σ_B is the plane-wave Born cross section (PWB). The scaling factor $E + B + E_{th}$ reduces Born cross sections at low energy while keeping the validity of the Born approximation intact at high E and also provides the correct order of magnitude for the cross section. The PWB cross sections for the rotational transition from $J = 0$ to $J' = 1$ is obtained using the expression [51]

$$\sigma_B = \frac{8\pi}{3k_i^2} D^2 \ln \left| \frac{k_i + k_f}{k_i - k_f} \right|, \quad (20)$$

where D is the dipole transition moment (in a.u.) for the ground to excited state; k_i (k_f) is the initial (final) momentum of the impinging positron.

The BE-scaling method does not account for the resonances if any distortion of the plane waves in the vicinity of the target and the target polarization due to the incident positron. Furthermore, the scaling approach applies only to the integrated excitation cross sections and not to their angular distributions, as it does not alter the shape of the angular distribution as described by the unscaled Born cross sections.

D. Total cross sections

The total positron scattering cross sections, TCS (Q_T), are needed in many areas of applied physics and also serve as a check on theoretically determined cross sections. The TCS is the sum of the cross sections for all scattering channels available to the projectile like the elastic scattering, vibrational,

positronium formation, ionization, annihilation and excitation, etc. [24]. The contribution of annihilation cross sections to TCS is always negligible except in the limit of zero positron energy [23]. The double ionization cross sections are also very small [52]. The modeling of Ps formation is challenging as its cross sections depend on the molecular structure like dipole polarizability of target [53]. This channel can be modeled using the molecular CCC approach [23,54]. The BEB model cannot consider the rearrangement channel along with the direct scattering simultaneously. This channel was therefore omitted and the remaining channels were summed incoherently to estimate the TCS:

$$Q_T = Q_e + Q_v + Q_I + Q_{ex}. \quad (21)$$

III. TARGET DESCRIPTION, METHODOLOGY, AND COMPUTATIONAL DETAILS

The molecular geometry of 1,1-difluoroethylene was referred from NIST [28] and was optimized at the HF level by employing the cc-pVTZ basis set using Gaussian software (version 03) [55]. It is a closed-shell molecule and belongs to the C_{2v} point group. Its ground-state electronic configuration $1a_1^2 \dots 8a_1^2, 1b_1^2, 2b_1^2, 1b_2^2, 2b_2^2 \dots 5b_2^2, 1a_2^2$ corresponds to 1A_1 molecular symmetry.

The SCALIB code [56] was used to calculate the one-particle electron density and the potentials from the numerical SCE wave function. This code works at the HF level and is applicable to closed-shell molecules only. The expansion of bound-state quantities like wave function, density, and potential was carried out at the center of mass (c.m.) of the molecule up to l_{\max} , the maximum value of l . The parameter l represents the number of multipoles included in the expansion of bound-state molecular properties. The isotropic value of polarizability was obtained from Gaussian software to compute V_{cp} in the absence of its experimental value. The l_{\max} was taken as 50 for the bound-state wave function. The radial step for integration was kept to a fine but fixed mesh with a step size of 0.005 a.u. The large value of l_{\max} helped in ensuring orbitals are normalized to unity or at least get close to unity. The quadrature grid was chosen so that the SCE wave function was normalized and yielded a value of dipole moment, which was in agreement with the HF value obtained using Gaussian software. The elastic scattering calculations were performed using the POLYDCS code [47]. The quantities like B , U , and N , the frequency of the mode, and the infrared absorption intensity were obtained using Gaussian software. These quantities were required to compute BEB and vibrational cross sections. The BEB input parameters like B , U , and N are listed in Table I.

IV. RESULTS AND DISCUSSION

The present study provides a comprehensive set of positron impact cross sections over a wide energy range. The order of presentation of results is as follows: the ECS are presented first, followed by inelastic, TCS, DCS, and finally the MTCS. The observation from the comparative evaluation of the angular discrimination effect of the two spectrometers is presented at the end.

TABLE I. BEB input parameters obtained using a cc-pVTZ basis set at the HF level.

Molecular orbital	Binding energy ($ B $) (a.u.)	Kinetic energy (U) (a.u.)	Occupation number (N)
1b ₂	26.34711	37.23624	2
1a ₁	26.34708	37.23661	2
1a ₁	11.42136	16.02726	2
1a ₁	11.23086	16.01219	2
1a ₁	1.72107	3.50194	2
1b ₂	1.64895	3.88044	2
1a ₁	1.07522	1.95128	2
1a ₁	0.89616	2.68652	2
1b ₂	0.81510	2.81900	2
1b ₁	0.77385	2.64973	2
1a ₁	0.75727	2.33027	2
1a ₂	0.69360	3.24901	2
1b ₂	0.67091	3.30795	2
1a ₁	0.63819	2.21096	2
1b ₂	0.59636	1.29842	2
1b ₁	0.39055	1.48395	2

The Born correction for polar VDF was computed in BF and LAB frames cross sections using different schemes. The correction was carried out at the experimental value of dipole moment 0.543 a.u. [28]. Both correction schemes yielded similar results. The Born corrected ECS were compared with the experimental TCS of Makochekanwa *et al.* up to Ps formation, i.e., 3.5 eV. As expected, the Born corrected SCE-ECS were substantially higher than the experimental data of Makochekanwa *et al.*, which did not account for corrections due to forward scattering effects.

The linear-transmission technique-based spectrometers used for measuring positron impact elastic and total cross sections suffer from the forward angle discrimination effect. These spectrometers have the inherent limitation that they cannot measure scattering angle beyond a certain value known as the critical angle (θ_c). This θ_c is a spectrometer dependent quantity [57,58]. The effects of forward scattering are more profound for polar molecules at low energies and small scattering angles. They may extend to a higher energy range depending upon the strength of the dipole moment. As a consequence of the forward angle discrimination effect, the measured cross sections are always underestimated. Thus all experimental measurements are corrected before making any meaningful comparison with other results. The corrections are carried out using a theoretical approach. The presently available correction methods are DCS dependent and require energy-dependent critical data of the spectrometer. This important data is unavailable for several polar molecules [29]. As a result, these prescribed methods cannot be applied to correct the data. The Born top-up approach offers an alternative to the DCS based correction methods and was applied to correct the experimental data of Makochekanwa *et al.* The correction not only enhanced the magnitude of TCS but the theoretically corrected experimental results also got superimposed with the Born corrected SCE results up to Ps formation. The Born top-up method can be easily extended to other polar molecules for which uncorrected data exists. The DCS offers a more stringent test to evaluate any scattering model. Any technique involving their use is always difficult to implement. The Born

top-up correction approach is an easier approach to correct the experimental data. However, no correction is required for experimentally measured Ps or excitation cross sections for any kind of target (polar or nonpolar) [29,30].

A comparison was also made between the uncorrected SCE-ECS and experimental TCS of Makochekanwa *et al.* up to Ps formation. This is also shown in Fig. 1(a). The two different sets of uncorrected data are also in excellent agreement with each other from 0.6 eV onwards. This is not a fortuitous result. The same was also observed in positron scattering from acetone [59]. The trends below 0.6 eV in TCS of Makochekanwa *et al.* are not in conformity with the polar nature of a molecule and may be attributed to the limitations of the spectrometers used by them. In Fig. 1(b), we have displayed the Born corrected ECS up to 5 keV. The impact of polar nature on cross sections ceases beyond 100 eV. The uncorrected elastic cross sections are virtually flat from 2 to 30 eV.

Additional calculations were also performed at the HF level using a 6-311G* basis set to examine the uncertainty in the ECS obtained from the cc-pVTZ basis set. Beyond 0.8 eV, both basis sets give overlapping elastic cross sections.

For an infrared active mode of vibration, the Born approximation is often applied to estimate the vibrational cross sections (VCS) [60]. The cross sections due to positron-impact excitation of each infrared active mode of vibrations were summed to obtain the vibrational cross sections [61]. The magnitude of these cross sections is very small due to their nonresonant nature even at low energies. The results are displayed in Fig. 1(a).

The onset of open channels begins with Ps formation at 3.5 eV. The threshold for the electronic excitation and direct ionization is around 7 eV and 10.3 eV [28], respectively. The direct ionization cross sections obtained using the BEB model are plotted in Fig. 2(a). The maxima in the BEB model occurs at 85 eV, having a magnitude of 6.85 Å². The BEB cross sections increase from the threshold to about 85 eV and then fall in accordance with the $\log E/E$ term. There is no data available to compare the present results. The BEB ionization

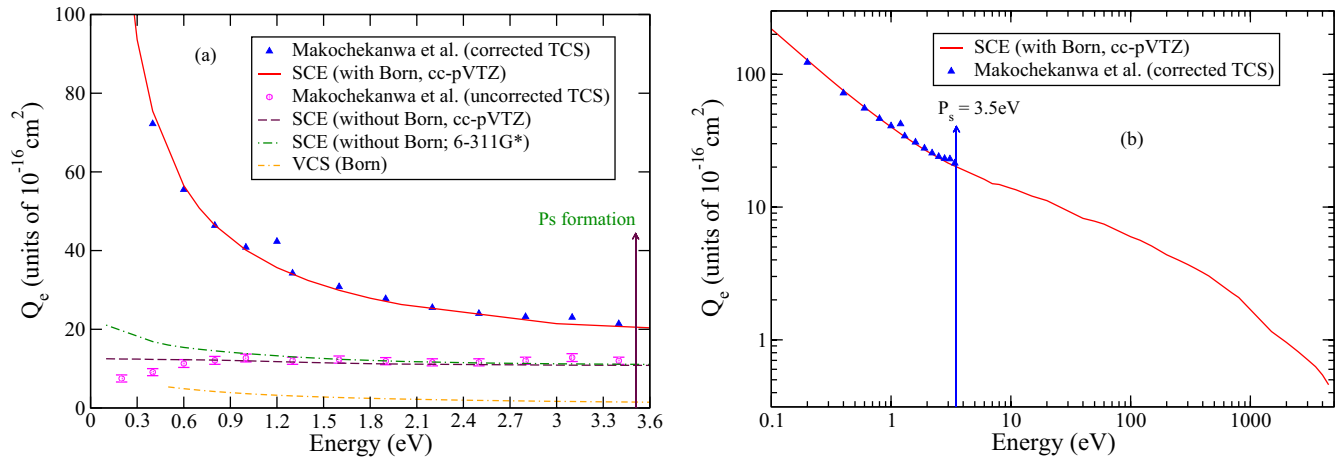


FIG. 1. Elastic cross sections: (a) line curve, Born corrected ECS up to 3.5 eV using cc-pVTZ basis sets; dashed curve, Born uncorrected ECS; dotted dashed curve, Born uncorrected ECS using 6-311G* basis set; triangles, forward angle corrected TCS of Makochekanwa *et al.* [5]; circles, forward angle uncorrected TCS of Makochekanwa *et al.*; dashed curves with dots, vibrational cross sections (VCS) in Born approximation. (b) Born corrected elastic cross sections up to 5 keV.

cross sections for positron are always higher than electron due to the exclusion of exchange and interference effects [36]. The same is noticed from Fig. 2(a) after plotting the BEB results for positrons and electrons [2]. This comparison provides a useful self-consistency check in the absence of any other data. The overlapping of both BEB curves beyond 350 eV indicates that the trends are independent of the projectile's charge.

The electronic excitation spectra of VDF show that the lowest two excited states are triplets [62]. In the case of positron scattering, the spin changing cross sections are strictly forbidden as they have a distinct identity with respect to the electron. However, the excitation of spin-allowed transitions must be considered since these cross sections may be substantial if the transition moment from the ground state to any excited state is significant. Assuming that the Born approximation is valid beyond 20 eV, we can estimate excitation cross sections by employing a scaled-BE approach [37]. The lowest two singlets' excited states, namely a^1B_1 and b^1A_1 ,

were considered for computing BE-scaled excitation cross sections. The experimental values of excitation thresholds [62] were used in the calculation. The relevant data is given in Table II. The BE-scaled excitations' cross sections (Q_{ex}) and their sum are displayed in Fig. 2(b). The Born approximation excludes the contribution of correlation effects which are essential at low energies and near the thresholds. These effects start diminishing as the projectile energy increases. Thus the use of Born approximation may introduce some uncertainties near the threshold region.

The elastic and inelastic cross sections were summed incoherently to obtain Q_T . A comparison was made with the forward angle corrected experimental results of Makochekanwa *et al.* The results are displayed in Fig. 3. We observe an extremely encouraging agreement between the two results barring a deviation in the 4–30 eV energy range. This is due to the exclusion of the Ps channel. The summed cross section data is also in agreement with the recommendations

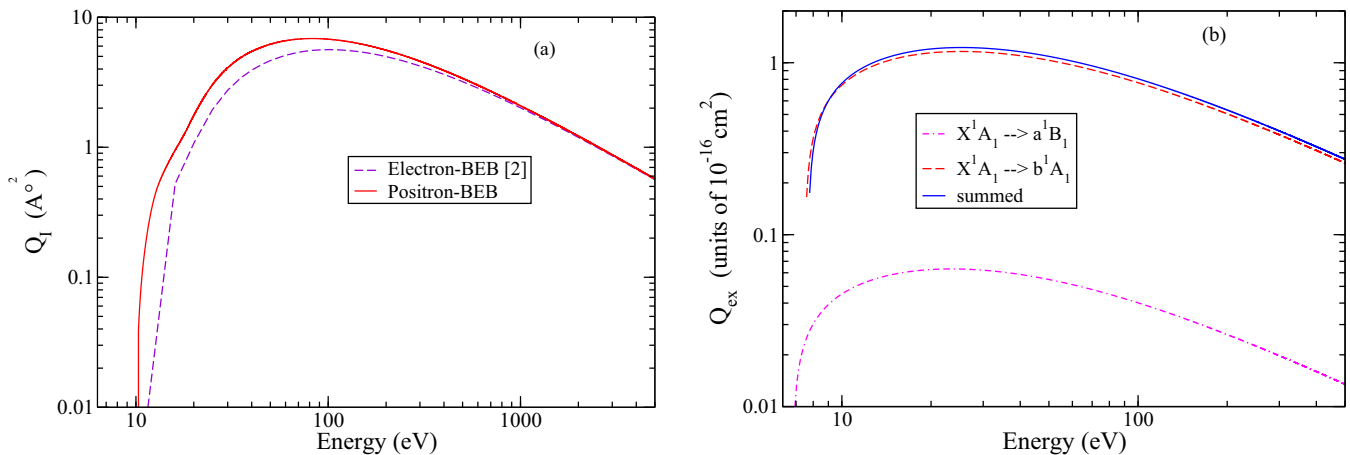


FIG. 2. (a) BEB ionization cross sections: line curve, positron; dashed curve, electron [2]. (b) BE scaled excitation cross sections: dashed dotted curve, $X^1A_1 \rightarrow a^1B_1$; dashed curve, $X^1A_1 \rightarrow b^1A_1$; line curve, summed excitation.

TABLE II. Important target parameters.

Ionization energy	Ps	Dipole moment	Polarizability ^a	First Excitation Threshold and Transition moment (³ A ₁)	First excitation threshold and transition moment of ¹ B ₁	Second excitation threshold and transition moment and of ¹ A ₁
10.30 eV [28]	3.5 eV	0.543 a.u. ^b [28] 0.489 ^a (HF), 0.49 (SCE)	23.06a ₀ ³	4.60 eV [62] 5.715 eV [2]	6.7–6.9 eV ^b , 0.336 a.u. [62]	7.5–7.6 eV ^b , 1.302 a.u. [62]

^aFrom Gaussian.

^bExperimental value.

of Brunger *et al.* [29], who have endorsed the experimental measurements of Makochekanwa *et al.* from 30 eV onwards. In the same figure, we have also shown the cross section data obtained by summing only the elastic and BEB cross sections. The results suggest that, beyond 30 eV, the contribution of Ps and excitation cross sections is substantially reduced, and the TCS can be estimated from elastic and direct ionization cross sections.

The understanding of angular dependence with an incident energy of projectile constitutes an important part of collision study. In Figs. 4 and 5, the Born corrected DCS are plotted at different energies ranging from 0.1 to 100 eV. The Born corrected DCS are moderately peaked in the forward direction due to the weak polar nature of the target. Also, the DCS are closely spaced. The long-range interactions dominate the forward angle scattering at lower energies ($E < 2$ eV). At higher energies, the short-range interactions become prominent. A sharp dip around 4° between 5 and 70 eV energy region is due to the change in dominance of long- and short-range interactions. At 100 eV, the polar nature diminishes.

Consequently, the correction becomes insignificant and the dip disappears. The short-range interactions would be sufficient to describe the angular distribution, i.e., the BF-DCS. We have also shown BF-DCS at 5 eV, 100 eV, and 200 eV in Figs. 4(b) and 5(b), respectively, to get an idea about the impact of the correction term on DCS. Another feature

of the angular distribution curve is its oscillatory nature at large scattering angles and higher energy ranges. This type of behavior was also noticed in electron scattering from VDF [2] and positron scattering from pyrimidine [63]. Both these studies were performed using POLYDCS code. The genesis of this oscillatory nature is the lack of convergence of the partial wave contributions originating from the term $A_L^B P_L(\cos\theta)$ in POLYDCS [64,65]. The impact of closely spaced DCS on elastic cross sections is very much visible on ECS.

The Born corrected, and uncorrected MTCS are shown in Fig. 6 from 0.1 to 0.1 keV. These cross sections are smooth and monotonically decrease with an increase in energy. The merging of Born corrected and uncorrected MTCS after 4 eV indicates that the domination of long-range dipole interaction is confined only up to 4 eV.

The two linear-transmission type spectrometers at the Universities of Trento [57] and ANU [58] used to perform positron scattering measurements employ different schemes to compute missing angular range data [29]. It is therefore equally important to evaluate their respective correction data. The angular discrimination of the Trento spectrometer varies between 71.68° at 0.1 eV positron energy to 2.48° at 50 eV [57]. The critical angles of the ANU spectrometer were computed at the retarding potential of 76.5 meV. The correction cross sections were obtained for these instruments using the Born top-up procedure. The results do not reveal any major change in their correction cross sections. It implies that the estimates for the angular discrimination and subsequent correction arising from the angular discrimination from both these spectrometers compare very well. The minor variations are due to their different critical angles, which depend upon the configuration and working of the spectrometers. The corrections were computed over a full angular range, i.e., θ varying from 0 to 180° using the Born top up to correct the ECS. The correction cross sections resulting from different angular ranges are very close to each other. This gives credence to our approach of obtaining the correction cross sections in the absence of the availability of angular data of the spectrometer used to measure the scattering cross sections. These results are plotted in Fig. 7.

Some important inferences are made from the work as follows.

The SCALIB code computes the molecular properties using the SD-HF wave function only for close shell targets. This method can only explain the positron scattering at the static level. The polarization effects are important at low energies and small scattering angles. A correct formulation of projectile-target interaction assumes importance in order to have a good agreement with the experimental results,

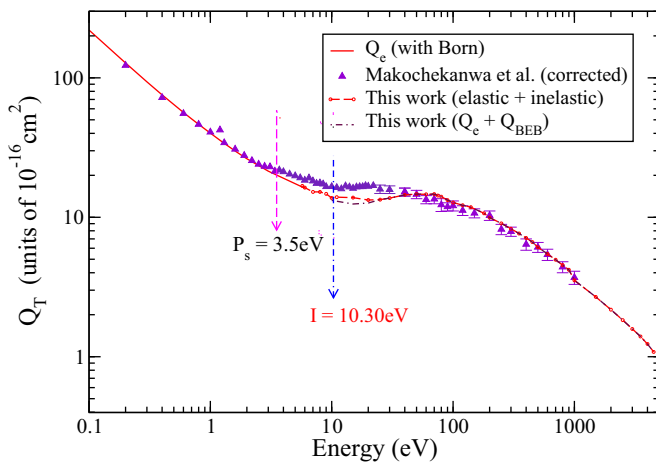


FIG. 3. Total cross sections: solid line, this work (below Ps); dashed line curve with circles, total (elastic and inelastic), this work; dotted dashed curve, elastic + ionization; triangles, forward angle corrected TCS of Makochekanwa *et al.* [5].

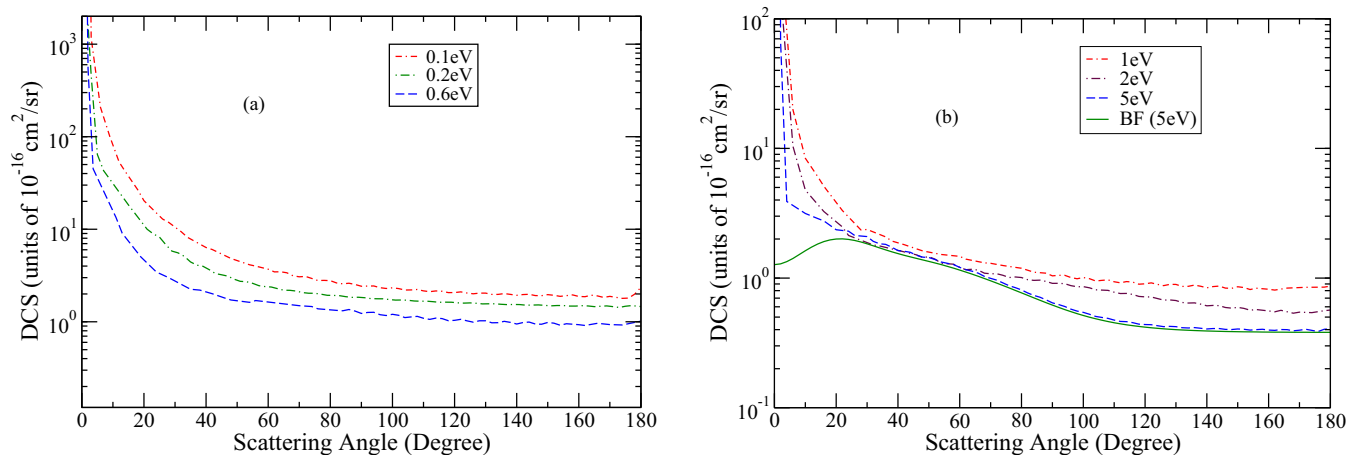


FIG. 4. Born corrected elastic DCS. (a) Dashed dotted curve, 0.1 eV; dotted dashed curve, 0.2 eV; double dashed curve, 0.6 eV. (b) Dashed curve, 1 eV; dotted dashed curve, 2 eV; dashed curve, 5 eV; line curve, BF-DCS at 5 eV.

especially if the projectile happens to be a positron. The explicit inclusion of the correlation-polarization potential using a model potential and static potential can yield reliable elastic scattering results with a substantial reduction of computational resources and time. An *ab initio* treatment to describe complete positron scattering from difluoroethylene or any target, from low to high energy, is the two-center expansion of total wave function and would require enormous computational resources. Even then, there are chances of calculations becoming intractable. Also, the CC calculations may suffer from the problem of ill conditioning [23–25,54] or linear dependence [66,67]. The approach to determine each channel separately and then sum them incoherently appears attractive to study positron scattering over an extended energy range. It is also free from the above problems. Present and earlier scattering results from acetone [59] give us the confidence to conclude that the present approach can provide reliable estimates of scattering data for any complex target. The Ps modeling would surely benefit the current approach.

Correction to elastic or total cross sections for polar molecules is an important aspect of any collision study. These corrections arise from the experimental and theoretical limitations. The theoretical treatment of elastic scattering within FNA leads to divergence in the elastic DCS for polar molecules in the forward direction due to lack of convergence in the partial wave expansion for large L . A variety of correction procedures also exist to overcome this problem [35,68,69]. In the present study, we have applied two different schemes to correct the theoretical data. The corrections to experimental measurements are necessary to overcome the angular limitations of the measuring instruments. The Born top-up procedure can be reliably invoked to correct both the theoretical and experimental data. The work also establishes that there is no major variation in the correction data of the spectrometers at the Universities of Trento and ANU.

The energy-dependent corrections are very sensitive to the value of dipole moment. The theoretical value of dipole moment depends on the choice of basis set and theory level (HF

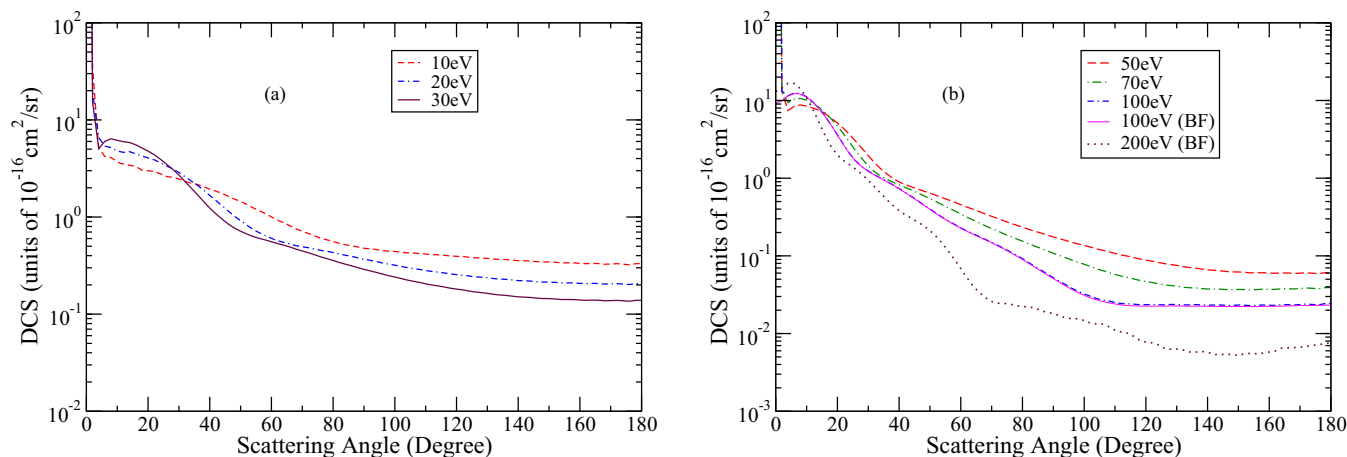


FIG. 5. Born corrected elastic DCS at different energies. (a) Dashed curve, 10 eV; dashed dotted curve, 20 eV; line curve, 30 eV. (b) Dashed curve, 50 eV; dotted dashed curve, 70 eV; dashed dotted curve, 100 eV; line curve, 100 eV (CC); dotted curve, 200 eV (BF).

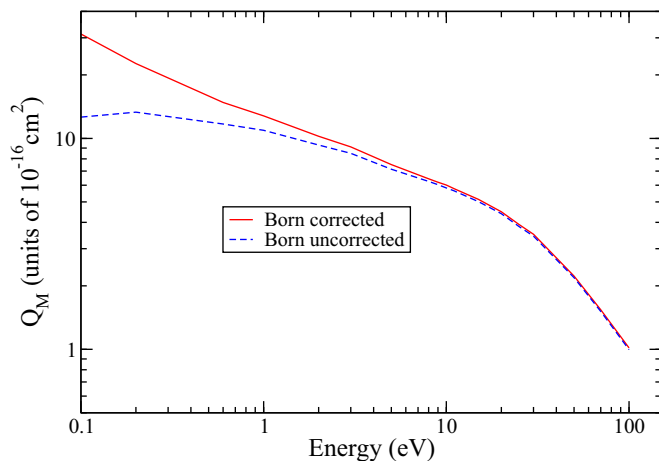


FIG. 6. MTCS up to 5 keV; line curve, Born corrected; dashed curve, Born uncorrected.

or DFT or MP2, etc.). Different values of dipole moment on account of theoretical methods, basis set, or experiment would give different correction and corrected cross sections [59]. To avoid this and for a better consistency, we used reference experimental value of dipole moment. This way the scattering results become independent of the MP3 or HF level. This is precisely the approach that we have followed in the study. An excellent agreement between the theoretical and forward angle corrected experimental cross sections results at energies below Ps formation in the present, and an earlier study [59] is an outcome of this approach.

In contrast to electron scattering, the positron-impact ionization can happen either through direct knocked-out ionization or through electron capture to the continuum (ECC) process. This means the knocked-out electron is either in the continuum state of the parent residual ion or in the continuum state of the electron-positron system, that is, of the Ps. As there is no way to separate the two ionizing processes, the

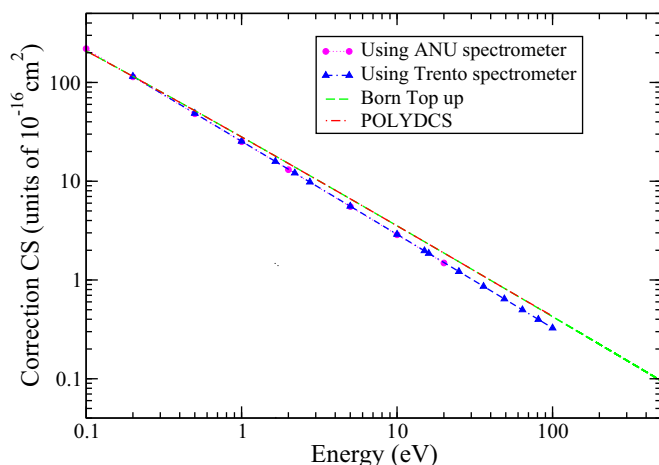


FIG. 7. Evaluation of correction cross sections (CS); dotted lines with circles, ANU spectrometer; triangles with dashed lines, Trento spectrometer. Full angular range: double dashed curve, Born top up; dotted dashed curve, POLYDCS.

final-state wave function must contain the proper asymptotic form arising out of both these collision processes. This can be done for a three-body collision process but is beyond the scope of the BEB model. The impact of Ps on scattering can be gauged in a very crude way. The peak for Ps and BEB cross sections occurs at different energies. It is generally around 27 eV due to Ps formation [29,70] and 85 eV in present BEB cross sections. The inelastic cross sections show falling trends with increased energy of projectile after the peak. Thus the trends in cross sections due to Ps and BEB are reversed in the energy region from 30 eV onwards. This would lead to an improved agreement between the experimental and theoretical TCS obtained by omitting the Ps channel at higher energies. The same is observed in this study beyond 30 eV.

V. CONCLUSIONS

Positron-molecule interactions are complex due to strong electron-positron correlations and the positronium formation channel. It makes positron scattering more challenging to model than electron scattering. The multicenter nature of molecules and additional degrees of freedom makes positron scattering a formidable task compared to atoms. This paper has reported various types of cross sections for positron impact on the 1-1- $C_2H_2F_2$ molecule in a straightforward yet efficient manner from low- to high-energy range. This approach would be helpful to study the scattering problem from the many-electron molecular systems, which may be challenging to treat using perturbative methods. Analysis of the scattering based on spectrometers at Trento University and ANU reveals that the angular discrimination of these spectrometers compares very well with each other. A Born top-up procedure can be used to overcome the limitations posed by spectrometers in providing the correct estimates of cross sections for polar molecules. The same approach can also be applied to include long-range interactions arising out of the nonzero dipole moment. The comparison with electron scattering forms a valuable part of the study to gain additional insight into the scattering process. This work would be immensely useful in positron plasma and transport modeling. The study is expected to motivate scientists to validate the data for processes studied for the first time. We hope that various research groups come up with a simple formulation to estimate the positronium contribution and its contribution to total cross sections.

ACKNOWLEDGMENTS

The authors V.S. and A.B. are grateful to the Department of Science and Technology, Government of India, and the Principal of Bhaskaracharya College of Applied Sciences for motivating the students and teachers to carry out this research work under the Star College Scheme.

All the authors were involved in the preparation of the manuscript and have read the final manuscript.

- [1] ECETOC JACC Report No. 49, European Centre for Ecotoxicology and Toxicology of Chemicals, Belgium, 2005.
- [2] M. Bassi, A. Bharadvaja, and K. L. Baluja, *Eur. Phys. J. D* **74**, 232 (2020).
- [3] K. C. Rao, K. G. Bhushan, S. C. Gadkari, M. Vinodkumar, and K. Korot, *J. Electron Spectrosc. Relat. Phenom.* **222**, 133 (2018).
- [4] M. D. Gurung and W. M. Ariyasinghe, *Nucl. Instrum. Methods, Phys. Res. B* **395**, 24 (2017).
- [5] C. Makochekanwa, H. Kato, M. Hoshino, M. H. F. Bettega, M. A. P. Lima, O. Sueoka, and H. Tanaka, *J. Chem. Phys.* **126**, 164309 (2007).
- [6] G. Sarri *et al.*, *Nat. Commun.* **6**, 6747 (2015).
- [7] S. Marjanović, A. Banković, D. Cassidy, B. Cooper, A. Deller, S. Dujko and Z. Lj. Petrović, *J. Phys. B: At., Mol., Opt. Phys.* **49**, 215001 (2016).
- [8] W. J. Tattersall, D. G. Cocks, G. J. Boyle, M. J. Brunger, S. J. Buckman, G. García, Z. L. Petrović, J. P. Sullivan, and R. D. White, *Plasma Sources Sci. Technol.* **26**, 045010 (2017).
- [9] G. J. Boyle, W. J. Tattersall, D. G. Cocks, S. Dujko, and R. D. White, *Phys. Rev. A* **91**, 052710 (2015).
- [10] F. Blanco *et al.*, *J. Phys. B: At., Mol., Opt. Phys.* **49**, 145001 (2016).
- [11] F. Blanco, A. Muñoz, D. Almeida, F. Ferreira da Silva, P. Limão-Vieira, M. C. Fuss, A. G. Sanz, and G. García, *Eur. Phys. J. D* **67**, 199 (2013).
- [12] A. G. Sanz, M. C. Fuss, A. Muñoz, F. Blanco, P. Limão-Vieira, M. J. Brunger, S. J. Buckman, and G. García, *Int. J. Radiat. Biol.* **88**, 71 (2012).
- [13] N. Guessoum, *Eur. Phys. J. D* **68**, 137 (2014).
- [14] R. L. Wahl and J. W. Buchanan, *Principles and Practice of Positron Emission Tomography* (Lippincott Williams and Wilkins, Philadelphia, PA, 2002).
- [15] L. D. Hulett, Jr., D. L. Donohue, J. Xu, T. A. Lewis, S. A. McLuckey, and G. L. Glish, *Chem. Phys. Lett.* **216**, 236 (1993).
- [16] P. J. Schultz and K. G. Lynn, *Rev. Mod. Phys.* **60**, 701 (1988).
- [17] M. C. Zammit, D. V. Fursa, and I. Bray, *Phys. Rev. A* **90**, 022711 (2014).
- [18] M. S. Pindzola *et al.*, *J. Phys. B: At., Mol., Opt. Phys.* **40**, R39 (2007).
- [19] R. Zhang, K. L. Baluja, J. Franz, and J. Tennyson, *J. Phys. B: At., Mol., Opt. Phys.* **44**, 035203 (2011).
- [20] R. Zhang, P. G. Galiatsatos, and J. Tennyson, *J. Phys. B: At., Mol., Opt. Phys.* **44**, 195203 (2011).
- [21] R. Utamuratov, D. V. Fursa, A. S. Kadyrov, and I. Bray, *Phys. Rev. A* **100**, 042703 (2019).
- [22] R. Utamuratov, D. V. Fursa, N. Mori, A. S. Kadyrov, I. Bray, and M. C. Zammit, *Phys. Rev. A* **99**, 042705 (2019).
- [23] A. S. Kadyrov and I. Bray, *J. Phys. B: At., Mol., Opt. Phys.* **49**, 222002 (2016).
- [24] M. C. Zammit, D. V. Fursa, J. S. Savage, and I. Bray, *J. Phys. B: At., Mol., Opt. Phys.* **50**, 123001 (2017).
- [25] I. Bray *et al.*, *J. Phys. B: At., Mol., Opt. Phys.* **50**, 202001 (2017).
- [26] N. A. Mori *et al.*, *J. Phys. B: At., Mol., Opt. Phys.* **53**, 015203 (2020).
- [27] K. Ratnavelu, M. J. Brunger, and S. J. Buckman, *J. Phys. Chem. Ref. Data* **48**, 023102 (2019).
- [28] <http://cccbdb.nist.gov>.
- [29] M. J. Brunger, S. J. Buckman, and K. Ratnavelu, *J. Phys. Chem. Ref. Data* **46**, 023102 (2017).
- [30] J. P. Sullivan *et al.*, *J. Phys. B: At., Mol., Opt. Phys.* **44**, 035201 (2011).
- [31] A. Loreti, R. Kadokura, S. E. Fayer, Á. Kövér, and G. Laricchia, *Phys. Rev. Lett.* **117**, 253401 (2016).
- [32] C. Makochekanwa, A. Banković, W. Tattersall, A. Jones, P. Caradonna, D. S. Slaughter, K. Nixon, M. J. Brunger, Z. Lj. Petrović, J. P. Sullivan, and S. J. Buckman, *New J. Phys.* **11**, 103036 (2009).
- [33] N. Sanna and F. A. Gianturco, *Comput. Phys. Commun.* **128**, 139 (2000).
- [34] F. A. Gianturco, R. R. Lucchese, N. Sanna and A. Talamo, A generalized single center approach for treating electron scattering from polyatomic molecules, in *Electron Collisions with Molecules, Clusters and Surfaces*, edited by H. Ehrhardt and L. A. Morgan (Plenum, New York, 1994).
- [35] I. Fabrikant, *J. Phys. B: At., Mol., Opt. Phys.* **49**, 222005 (2016).
- [36] K. Fedus and G. P. Karwasz, *Phys. Rev. A* **100**, 062702 (2019).
- [37] Y. K. Kim, *J. Chem. Phys.* **126**, 064305 (2007).
- [38] D. Raj, *J. Phys. B: At., Mol., Opt. Phys.* **24**, L431 (1991).
- [39] J. P. Perdew and A. Zunger, *Phys. Rev. B* **23**, 5048 (1981).
- [40] F. A. Gianturco and A. Jain, *Phys. Rep.* **143**, 347 (1986).
- [41] K. L. Baluja, N. J. Mason, L. A. Morgan, and J. Tennyson, *J. Phys. B: At., Mol., Opt. Phys.* **33**, L677 (2000).
- [42] K. L. Baluja, N. J. Mason, L. A. Morgan, and J. Tennyson, *J. Phys. B: At., Mol., Opt. Phys.* **34**, 4041 (2001).
- [43] K. L. Baluja, N. J. Mason, L. A. Morgan, and J. Tennyson, *J. Phys. B: At., Mol., Opt. Phys.* **34**, 2807 (2001).
- [44] S. Kaur, K. L. Baluja, and J. Tennyson, *Phys. Rev. A* **77**, 032718 (2008).
- [45] A. Bharadvaja, S. Kaur, and K. L. Baluja, *Phys. Rev. A* **91**, 032701 (2015).
- [46] A. Bharadvaja, S. Kaur, and K. L. Baluja, *Pramana* **89**, 30 (2017).
- [47] N. Sanna and F. A. Gianturco, *Comput. Phys. Commun.* **114**, 142 (1998).
- [48] H. Klar, *J. Phys. B: At., Mol., Opt. Phys.* **14**, 4165 (1981).
- [49] Y.-K. Kim and M. E. Rudd, *Phys. Rev. A* **50**, 3954 (1994).
- [50] R. Utamuratov, A. S. Kadyrov, D. V. Fursa, M. C. Zammit, and I. Bray, *Phys. Rev. A* **92**, 032707 (2015).
- [51] Y. Itikawa, *Molecular Processes in Plasmas Collisions of Charged Particles with Molecules*, Springer Series on Atomic, Optical, and Plasma Physics Vol. 43 (Springer, Berlin, 2007).
- [52] D. A. Cooke, D. J. Murtagh, Á. Kövér, and G. Laricchia, *Nucl. Instrum. Methods, B* **266**, 466 (2008).
- [53] J. R. Machacek, F. Blanco, G. García, S. J. Buckman, and J. P. Sullivan, *J. Phys. B: At., Mol., Opt. Phys.* **49**, 064003 (2016).
- [54] R. Utamuratov, D. V. Fursa, A. S. Kadyrov, I. B. Abdurakhmanov, and I. Bray, *J. Phys. B: At., Mol., Opt. Phys.* **54**, 095201 (2021).
- [55] M. J. Frisch, G. W. Trucks, H. B. Schlegel *et al.*, *Gaussian 03* (Gaussian Inc, Wallingford, CT, 2004).
- [56] N. Sanna, I. Baccarelli, and G. Morelli, *Comput. Phys. Commun.* **180**, 2544 (2009).
- [57] A. Zecca, L. Chiari, E. Trainotti, A. Sarkar, and M. J. Brunger, *PMC Phys. B* **3**, 4 (2010).
- [58] C. M. Surko, G. F. Gribakin, and S. J. Buckman, *J. Phys. B: At., Mol., Opt. Phys.* **38**, R57 (2005).

- [59] V. Sahgal, A. Bharadvaja, and K. L. Baluja, *J. Phys. B: At., Mol., Opt. Phys.* **54**, 075202 (2021).
- [60] Y. Itikawa, *J. Phys. B: At., Mol., Opt. Phys.* **37**, R1 (2004).
- [61] D. Gupta, K. L. Baluja, and Mi-Y. Song, *Phys. Plasmas* **26**, 063503 (2019).
- [62] S. Arulmozhiraja, M. Ehara, and H. Nakatsuj, *J. Chem. Phys.* **126**, 044306 (2007).
- [63] J. Franz and F. A. Gianturco, *Phys. Rev. A* **88**, 042711 (2013).
- [64] T. Meltzer, J. Tennyson, Z. Mašín, M. C. Zammit, L. H. Scarlett, D. V. Fursa, and I. Bray, *J. Phys. B: At., Mol., Opt. Phys.* **53**, 145204 (2020).
- [65] R. Zhang, A. Faure, and J. Tennyson, *Phys. Scr.* **80**, 015301 (2009).
- [66] J. Tennyson, *Phys. Rep.* **491**, 29 (2010).
- [67] Z. Mašín, J. Benda, J. D. Gorfinkiel, A. G. Harvey, and J. Tennyson, *Comput. Phys. Commun.* **249**, 107092 (2020).
- [68] R. O. Lima, G. M. Moreira, M. H. F. Bettega, and S. d'Almeida Sanchez, *J. Phys. Chem. A* **124**, 6790 (2020).
- [69] Y. Itikawa, *Theor. Chem. Acc.* **105**, 123 (2000).
- [70] M. Kimura, O. Sueoka, A. Hamada, and Y. Itikawa, in *Advances in Chemical Physics*, edited by I. Prigogine and S. A. Rice (John Wiley & Sons Inc., New York, 2000), p. 111.